

Generalized hierarchical bases for discontinuous Galerkin discretizations of elliptic problems with highly varying coefficients

J. Kraus, S. Margenov

RICAM-Report 2008-32

Generalized hierarchical bases for discontinuous Galerkin discretizations of elliptic problems with highly varying coefficients

J. Kraus*

S. Margenov†

Abstract

In this paper we present a new construction of generalized hierarchical bases (GHB) for symmetric positive definite matrices arising from discontinuous Galerkin discretization of second-order partial differential equations (PDE) with highly varying coefficients.

In the well-established theory of hierarchical basis multilevel methods one basic assumption is that the PDE coefficients are smooth functions on the elements of the coarsest mesh partition. However, as it is shown (for the two-level basis of the scalar elliptic problem), the newly developed GHB yields a robust splitting with respect to jump discontinuities of the PDE coefficient at arbitrary element interfaces on the finest mesh.

Though our focus is on a particular family of rotated bilinear finite elements in two space dimensions (2D) here, the proposed rather general approach is neither limited to this particular choice of elements nor to 2D problems. The presented numerical tests are in the spirit of algebraic multilevel iteration (AMLI) methods.

KEY WORDS: Discontinuous Galerkin methods, elliptic problems, hierarchical bases, highly varying coefficients, CBS constant.

1 Introduction

Optimal order algebraic multilevel iteration (AMLI) preconditioners based on recursive application of two-level finite element (FE) methods have been introduced and originally analyzed in context of linear conforming elements, see e.g., [4, 5]. The construction follows the natural hierarchical splitting using that the FE spaces corresponding to two successive mesh refinements are nested. The key role in the derivation of optimal convergence rate estimates plays the constant γ in the strengthened Cauchy-Bunyakowski-Schwarz (CBS) inequality, associated with the angle between the two subspaces induced by the hierarchical splitting. It turns out that existence only of a uniform estimate for this constant is not enough, but also accurate quantitative bounds for γ are required. More precisely, the value of the upper bound for $\gamma \in (0, 1)$ is a part of the construction of the multilevel extension of the related two-level method.

*Johann Radon Institute for Computational and Applied Mathematics, Austrian Academy of Sciences, Altenberger Straße 69, A-4040 Linz, Austria, johannes.kraus@oeaw.ac.at

†Institute for Parallel Processing, Bulgarian Academy of Sciences, Acad. G. Bonchev Bl. 25A, 1113 Sofia, Bulgaria, margenov@parallel.bas.bg

More recently, optimal order AMLI methods related to Crouzeix-Raviart and Rannacher-Turek nonconforming finite elements have been studied by different authors [6, 7, 15, 16, 21]. An important point to make is that in case of nonconforming discretizations the finite element spaces corresponding to two successive levels of mesh refinement are not nested in general. To handle this, a proper two-level basis is required. Previously developed multilevel methods for nonconforming elements are in the spirit of the standard (linear) and nonlinear AMLI methods for so called "First reduce" (FR) and "Differences and aggregates" (DA) hierarchical splittings.

In this paper we address AMLI preconditioners for linear algebraic systems obtained from interior penalty discontinuous Galerkin (IP-DG) finite element methods. In the case of scalar self-adjoint elliptic problems, the related stiffness matrix is symmetric and positive definite. Let us note that this is a special case of a more general class of DG schemes for second-order elliptic problems (see, e.g. [3, 9, 13]). Among the advantages of DG methods is that they are locally conservative which is of a principle importance for problems with highly varying coefficients. There are cited some first works on efficient solution methods for DG-FEM systems [8, 10, 11, 17, 22, 23].

Following the two-level approach from [10], a new class of AMLI methods for the resulting graph-Laplacian systems was proposed in [24]. In [22, 23] novel AMLI preconditioners have been introduced for IP-DG discretizations based on conforming elements. In this approach a sequence of algebraic problems is generated that can be associated with a hierarchy of coarse versions of DG approximations of the original problem. The obtained optimal complexity results are applicable in a rather general setting, e.g., they cover 2D and 3D, isotropic as well as anisotropic elliptic problems. In all these cases new concepts of local matrices are used to substitute the standard element stiffness matrices in the FEM assembling procedure.

The commonly known theory of optimal order solution methods for FEM elliptic systems is restricted to the case of coefficient jumps which are aligned with the coarse(st) mesh partitioning (triangulation). Such assumptions are usually made in case of multilevel, multigrid and domain decomposition methods. There are many numerical tests confirming that the convergence of these methods deteriorates if this condition is violated. However, at the same time, there are many (multiscale and multiphysics) models for strongly heterogeneous media where the strong coefficient jumps can be resolved on the finest mesh only! The hierarchical bases proposed in this paper are especially designed for problems with highly varying coefficients. The robustness issue we are investigating here concerns jump discontinuities of the PDE coefficient at arbitrary element interfaces (on the fine mesh). A hierarchical basis that provides a *robust splitting* (in this situation) yields a uniform upper bound (strictly less than one) of the CBS constant that measures the cosine of the abstract angle between the coarse space and its complementary space. Stochastically independent uniformly distributed random values of the diffusion coefficient are used to set the configuration of the test problem.

2 Rannacher-Turek finite elements

Non-conforming rotated multilinear finite elements were introduced by Rannacher and Turek [25] as a class of simple elements for stable discretization of the Stokes problem. Let \mathcal{T} be a regular decomposition of the domain $\Omega \subset \mathbb{R}^2$ into quadrilaterals denoted by T . The square $[-1, 1]^2$ is used as a reference element \hat{T} to define the isoparametric rotated bilinear element $T \in \mathcal{T}$. Let $\Psi_T : \hat{T} \rightarrow T$ be the corresponding bilinear bijective transformation. We set

$$Q_1(T) := \{q \circ \Psi_T^{-1} : q \in \text{span}\{1, x_1, x_2, x_1^2 - x_2^2\}\}.$$

For defining the required interpolation conditions let us denote by Γ^i the faces of a given element and by \mathbf{m}^i the midpoints of the faces. There are natural sets of nodal functionals:

- a) mean value (MV) continuity symbolized by the nodal functional $F_{\Gamma^i}^{\text{MV}}(\mathbf{v}) = |\Gamma^i|^{-1} \int_{\Gamma^i} \mathbf{v} d\Gamma^i$
- b) midpoint (MP) continuity symbolized by the nodal functional $F_{\Gamma^i}^{\text{MP}}(\mathbf{v}) = \mathbf{v}(\mathbf{m}^i)$

The corresponding finite element spaces are

$$\mathbf{W}_h^{\text{MV/MP}} := \left\{ \mathbf{v} \in [L_2(\Omega)]^d : \mathbf{v} \in Q_1(T) \forall T \in \mathcal{T}, \mathbf{v} \text{ is continuous w.r.t.} \right. \\ \left. \text{all the functionals } F_{\Gamma^i}^{\text{MV/MP}}, \text{ and } F_{\Gamma^i}^{\text{MV/MP}} = 0 \text{ if } \Gamma^i \subset \partial\Omega_D \right\}.$$

In [25] it is shown that \mathbf{W}_h^{MV} is less sensitive to mesh distortion than \mathbf{W}_h^{MP} when solving the Stokes problem, but that both spaces yield a stable discretization with respect to the Babuska-Brezzi condition. The space \mathbf{W}_h^{MV} , however, is also more natural for the DG formulation and we will therefore concentrate on discrete problems satisfying the mean value continuity condition.

3 Discontinuous Galerkin FE approximation of a scalar second-order elliptic problem

Consider the second-order elliptic boundary value problem on a polygonal domain $\Omega \subset \mathbb{R}^d$, $d = 2, 3$:

$$-\nabla \cdot (a(x)\nabla u) = f(x) \quad \text{in } \Omega \tag{1a}$$

$$u(x) = 0 \quad \text{on } \Gamma_D \tag{1b}$$

$$a\nabla u \cdot \mathbf{n} = 0 \quad \text{on } \Gamma_N. \tag{1c}$$

Here \mathbf{n} is the exterior unit normal vector to $\partial\Omega \equiv \Gamma$. The boundary is assumed to be decomposed into two disjoint parts Γ_D and Γ_N , $\Gamma_D \cap \Gamma_N = \emptyset$. For the formulation below we shall need the existence of the traces of u and $a\nabla u \cdot \mathbf{n}$ on certain interfaces in Ω . Thus, the solution u is assumed to have the required regularity. To simplify our exposition we assume that the set Γ_D is not empty and its \mathbb{R}^{d-1} -dimensional measure is nonzero.

Let \mathcal{T} be a partitioning of Ω into a finite number of open subdomains (finite elements) T with boundaries ∂T . We assume that the partition is quasi uniform and regular. For each finite element we denote by h_T its size and further $h = \max_{T \in \mathcal{T}} h_T$. Let $e = \overline{T^+} \cap \overline{T^-}$ be the interface of two adjacent subdomains T^+ and T^- (see Figure 1). The set of all such interfaces is denoted by \mathcal{F}_0 . Note that these interfaces are inside Ω . Further, \mathcal{F}_D and \mathcal{F}_N will be the sets of faces/edges of finite elements on the boundary Γ_D and Γ_N , respectively. Finally, \mathcal{F} will be the set of all faces/edges: $\mathcal{F} = \mathcal{F}_0 \cup \mathcal{F}_D \cup \mathcal{F}_N$. Here we allow finite elements of polygonal or polyhedral shape, with hanging nodes etc. The important assumption is that if e is a side or a face of a finite element $T \in \mathcal{T}$ then $|e| \approx h_T$ for $d = 2$ and $|e|^{\frac{1}{2}} \approx h_T$ for $d = 3$. In other words we do not allow very small edges or faces, i.e., strong mesh anisotropy is excluded.

On the partition \mathcal{T} we define the finite element space

$$\mathcal{V} := \mathcal{V}(\mathcal{T}) := \{v \in L^2(\Omega) : v|_T \in P_r(T), T \in \mathcal{T}\},$$

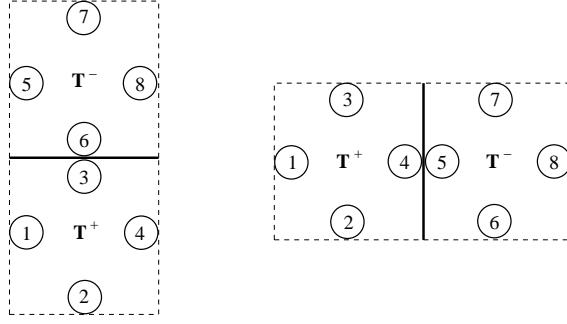


Figure 1: Degrees of freedom of face matrices: horizontal face (left) and vertical face (right)

where P_r is the set of polynomials of degree $r \geq 0$. For each $e = \bar{T}^+ \cap \bar{T}^- \in \mathcal{F}_0$ we define the jump $[[v]]$ of any function $v \in \mathcal{V}$ as the vector

$$[[v]]_e := \begin{cases} v|_{T^+} \cdot \mathbf{n}^+ + v|_{T^-} \cdot \mathbf{n}^-, & e = \bar{T}^+ \cap \bar{T}^-, \text{ i.e., } e \in \mathcal{F}_0, \\ v|_T \cdot \mathbf{n}, & e = \bar{T} \cap \Gamma_D, \text{ i.e., } e \in \mathcal{F}_D. \end{cases}$$

Here \mathbf{n}^+ and \mathbf{n}^- are the external unit vectors to T^+ and T^- , respectively. We shall also need the following notation for the average value of the traces of a vector function $\mathbf{v} \in \mathcal{V}$ on $e = \bar{T}^+ \cap \bar{T}^-$, that is,

$$\{\mathbf{v}\}_e := \begin{cases} \frac{1}{2}(\mathbf{v}|_{T^+} + \mathbf{v}|_{T^-}), & e = \bar{T}^+ \cap \bar{T}^-, \text{ i.e., } e \in \mathcal{F}_0, \\ \mathbf{v}|_T, & e = \bar{T} \cap \Gamma_D, \text{ i.e., } e \in \mathcal{F} \setminus \mathcal{F}_0 \end{cases}$$

and the piece-wise constant function $h_{\mathcal{F}}$ defined on \mathcal{F} as

$$h_{\mathcal{F}} = h_{\mathcal{F}}(x) = \begin{cases} |e|, & \text{for } x \in e \in \mathcal{F}, d = 2, \\ |e|^{\frac{1}{2}}, & \text{for } x \in e \in \mathcal{F}, d = 3. \end{cases}$$

Further denote by

$$(a \nabla v, \nabla v)_h := \sum_{T \in \mathcal{T}} \int_T a \nabla u \cdot \nabla v \, dx,$$

$$\langle h_{\mathcal{F}}^{-1} [[u]], [[v]] \rangle_{\mathcal{F}_0 \cup \mathcal{F}_D} := \sum_{e \in \mathcal{F}_0 \cup \mathcal{F}_D} \int_e h_{\mathcal{F}}^{-1} [[u]] \cdot [[v]] \, ds.$$

Finally, we introduce the broken norm

$$\|v\|_h^2 = (a \nabla v, \nabla v)_h + \alpha \langle h_{\mathcal{F}}^{-1} [[v]], [[v]] \rangle_{\mathcal{F}_0 \cup \mathcal{F}_D} \quad (2)$$

on \mathcal{V} .

Now let us consider the following symmetric interior penalty discontinuous Galerkin (IP-DG) finite element method (see, e.g. [3]): Find $u_h \in \mathcal{V}$ such that

$$\mathcal{A}_h(u_h, v) = (f, v), \quad \forall v \in \mathcal{V}, \quad (3)$$

where

$$\begin{aligned} \mathcal{A}_h(u_h, v) \equiv & (a\nabla u_h, \nabla v)_h + \alpha \langle h_{\mathcal{F}}^{-1} \llbracket u_h \rrbracket, \llbracket v \rrbracket \rangle_{\mathcal{F}_0 \cup \mathcal{F}_D} \\ & - \langle \{a\nabla u_h\}, \llbracket v \rrbracket \rangle_{\mathcal{F}_0 \cup \mathcal{F}_D} - \langle \llbracket u_h \rrbracket, \{a\nabla v\} \rangle_{\mathcal{F}_0 \cup \mathcal{F}_D}. \end{aligned} \quad (4)$$

It is well known that if α is sufficiently large then the bilinear form (4) is coercive and bounded on \mathcal{V} equipped with the norm (2), (see, e.g. [3]). We summarize the main results regarding the IP-DG method (3) in the following lemma:

Lemma 3.1 *Assume that the finite element partition \mathcal{T} is regular and locally quasi uniform. Then the bilinear form $\mathcal{A}_h(\cdot, \cdot)$ defined by (4) is coercive and bounded in \mathcal{V} equipped with the norm (2) for any sufficiently large $\alpha > 0$ and the discontinuous Galerkin method (3) has a unique solution.*

Note that the global stiffness matrix related to the bilinear form (4) can also be assembled from small-sized local stiffness matrices associated with the individual element faces $e \in \mathcal{F}$, i.e.,

$$A = \sum_{e \in \mathcal{F}} A_e$$

where summation is understood in the sense of the finite element assembling procedure. For an interior face $e \in \mathcal{F}_0$ the matrix A_e is then related to the local bilinear form

$$\begin{aligned} \mathcal{A}_e(u_h, v) \equiv & \frac{1}{2d} ((a\nabla u_h, \nabla v)_{T^+} + (a\nabla u_h, \nabla v)_{T^-}) + \alpha \langle h_{\mathcal{E}}^{-1} \llbracket u_h \rrbracket, \llbracket v \rrbracket \rangle_e \\ & - \langle \{a\nabla u_h\}, \llbracket v \rrbracket \rangle_e - \langle \llbracket u_h \rrbracket, \{a\nabla v\} \rangle_e. \end{aligned}$$

A simple computation shows that in the model case of a uniform mesh (composed of square elements) the matrices corresponding to the single contributions of horizontal and vertical (interior) faces have the representation

$$A_e^h = A_{e,0}^h + \alpha A_{e,1}^h, \quad (5)$$

$$A_e^v = A_{e,0}^v + \alpha A_{e,1}^v, \quad (6)$$

where the matrix terms from the r.h.s. of (5) can be written in the form

$$\begin{aligned} A_{e,0}^h &= \frac{1}{8} \begin{bmatrix} 5a^+ & -3a^+ & 3a^+ & a^+ & 0 & -6a^+ & 0 & 0 \\ -3a^+ & 5a^+ & -a^+ & -3a^+ & 0 & 2a^+ & 0 & 0 \\ 3a^+ & -a^+ & -15a^+ & 3a^+ & -6a^- & 10(a^+ + a^-) & 2a^- & -6a^- \\ a^+ & -3a^+ & 3a^+ & 5a^+ & 0 & -6a^+ & 0 & 0 \\ 0 & 0 & -6a^- & 0 & 5a^- & 3a^- & -3a^- & a^- \\ -6a^+ & 2a^+ & 10(a^+ + a^-) & -6a^+ & 3a^- & -15a^- & -a^- & 3a^- \\ 0 & 0 & 2a^- & 0 & -3a^- & -a^- & 5a^- & -3a^- \\ 0 & 0 & -6a^- & 0 & a^- & 3a^- & -3a^- & 5a^- \end{bmatrix}, \\ A_{e,1}^h &= \frac{1}{240} \begin{bmatrix} 23 & -3 & -3 & -17 & -23 & 3 & 3 & 17 \\ -3 & 3 & 3 & -3 & 3 & -3 & -3 & 3 \\ -3 & 3 & 243 & -3 & 3 & -243 & -3 & 3 \\ -17 & -3 & -3 & 23 & 17 & 3 & 3 & -23 \\ -23 & 3 & 3 & 17 & 23 & -3 & -3 & -17 \\ 3 & -3 & -243 & 3 & -3 & 243 & 3 & -3 \\ 3 & -3 & -3 & 3 & -3 & 3 & 3 & -3 \\ 17 & 3 & 3 & -23 & -17 & -3 & -3 & 23 \end{bmatrix}. \end{aligned}$$

Here the isotropic (scalar) coefficient $a = a(T)$ is defined by $a(T^\pm) = a^\pm$. Moreover, assuming a uniform mesh the vertical face matrix A_e^v is obtained from A_e^h via the following permutation of rows and columns:

$$A_e^v = S_{h,v}^t A_e^h S_{h,v},$$

where

$$(S_{h,v})_{i,j} = \begin{cases} 1 & \text{if } j = \mathbf{s}_i \\ 0 & \text{else} \end{cases}, \quad (7)$$

$$\mathbf{s} = (2, 1, 4, 3, 6, 5, 8, 7)^t$$

and the numbering of nodes belonging to horizontal and vertical faces is as shown in Figure 1.

Remark 3.1 For the considered particular case of a uniform mesh of square elements the analysis of the stabilization parameter shows that when $a^+ = a^-$ the condition of Lemma 3.1 is satisfied for $\alpha > \frac{\sqrt{23329} - 127}{8} \approx 3.22$.

4 Generalized hierarchical bases for the discrete problem

The decomposition of the DG-FE space into a coarse space and its complementary space on the discrete (matrix) level is based on a (generalized) hierarchical basis transformation that can be defined locally, i.e., for so-called macro superelements. We will describe the procedure for the scalar elliptic problem in detail. A generalization to systems of partial differential equations, such as the Lamé system of linear elasticity is straightforward.

The first step in the construction is related to a splitting of the local bilinear form into the contributions associated with the single horizontal and vertical (interior) faces in the mesh (see (5) and (6)).

In the next step we define a general so-called superelement $g \in \mathcal{G}$, which is the union of all the degrees of freedom (DOF) associated with the four faces (two horizontal and two vertical faces) that share one vertex, see Figure 2. The characteristic macro superelement $G \in \mathcal{M}$ is then made up

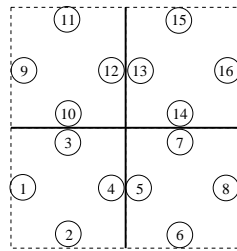


Figure 2: Superelement g composed of two horizontal and two vertical faces

of four partly overlapping superelements as shown in Figure 3. Note that the construction of faces, superelements and macro superelements is such that the global stiffness matrix can be assembled alternatively, in either way, of the respective local matrices, i.e.,

$$A = \sum_{e \in \mathcal{F}} A_e = \sum_{g \in \mathcal{G}} A_g = \sum_{G \in \mathcal{M}} A_G.$$

Due to the overlap of superelements a proper scaling of the respective face contributions is required when assembling superelement matrices. For an interior superelement g (none of its elements touches the boundary) the correct scaling factor is $1/2$, i.e., $A_g = \sum_{e \in g} \frac{1}{2} A_e$. The superelements can be associated with the (interior) vertices of the mesh, i.e., each vertex–intersection of (four interior) faces–defines one superelement and the coupling between the unknowns corresponding to different elements in a given superelement is due to the face matrices. The macro superelements finally cover the whole domain thereby forming stripes of overlap with a width of one element, see Figure 4. The overlapping region (intersection) of all four superelements of a macro superelement is one element in its center, i.e., the element with the local DOF (respectively nodes) 1, 2, 3, 4, as depicted in Figure 3. The DOF in the macro superelement G are divided into coarse DOF that belong to the corner elements – indicated by squares – and the remaining fine DOF – indicated by circles. As usual, the coarse DOF of a macro superelement form the DOF of a superelement on the next coarser level.

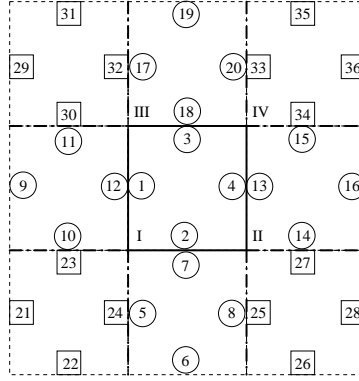


Figure 3: Macro superelement G : four overlapping superelements

The basic construction follows now from the standard approach, as it is used for conforming bilinear elements, if one associates nodes with elements. Hence, in the present context, we consider superelements g (instead of elements) in order to compose macro superelements G (instead of macro elements). Superelements produce overlapping (common) elements (instead of common nodes in the standard setting). Two ”neighboring” macro superelements have three elements in common, see Figure 4 (instead of having three common nodes in the standard situation of conforming bilinear elements). The coarse mesh hierarchy is such that the DOF associated with every other element (in x - and every other element in y -direction) belong to the coarse level. Since all DOF of a given element are either ”fine” or ”coarse”, the number of coarse DOF is always a multiple of four (in the scalar case). The number of elements that contain the coarse DOF is approximately reduced by a factor 4 in each coarsening step (for large meshes) and thus the ratio $\varrho := N^{(k+1)}/N^{(k)} \approx 4$ where $N^{(k+1)}$ and $N^{(k)}$ denote the number of DOF at levels $k + 1$ and k , respectively, see Figure 4. The macro superelement matrix associated with G is denoted by A_G ; It is transformed into a hierarchical two-level basis via a local transformation

$$\hat{A}_G = J_G^t A_G J_G \quad (8)$$

where J_G has the form

$$J_G = \begin{bmatrix} I & P_G \\ 0 & I \end{bmatrix} \quad (9)$$

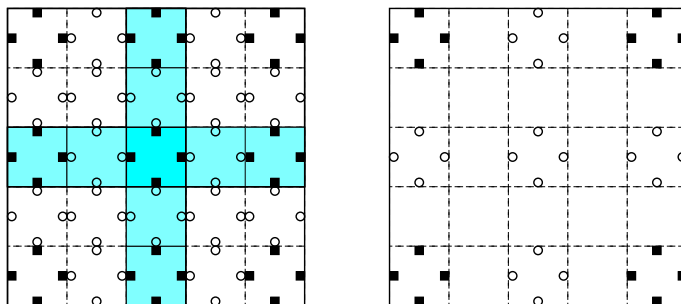


Figure 4: Overlap of macro superelements and coarsening

and P_G denotes some proper local interpolation matrix of size 20×16 (in the scalar case). Note that the local and global hierarchical bases, as presented here, do not involve so-called differences and aggregates of nodal shape functions. As opposed to the latter construction, which has turned out to be useful for splitting certain nonconforming FE spaces in a proper way, see, e.g., [7, 16, 21], we stay within the framework of nested spaces here.

4.1 Two-level splitting based on local energy minimization

In this section we show how to compute a local interpolation operator P_G such that the general transformation (9) provides a (local) minimum energy extension

$$\begin{bmatrix} P_G \\ I \end{bmatrix}$$

from the local coarse to the local fine space subject to global compatibility. We start with a so-called static condensation of the interior macro superelement DOF with local numbers 1, 2, 3, 4, see Figure 3. After this reduction step we arrive at a (in our case 32×32) local Schur complement

$$B_G = A_{G:22} - A_{G:21}A_{G:11}^{-1}A_{G:12}.$$

Here $A_{G:11}$ denotes the upper-left 4×4 submatrix corresponding to the interior DOF of G that are eliminated. This static condensation yields a local transformation into block diagonal form, i.e., a decoupling of the interior DOF from the remaining ones:

$$\begin{bmatrix} A_{G:11} & 0 \\ 0 & B_G \end{bmatrix} = \begin{bmatrix} I & 0 \\ -A_{G:21}A_{G:11}^{-1} & I \end{bmatrix} \begin{bmatrix} A_{G:11} & A_{G:12} \\ A_{G:21} & A_{G:22} \end{bmatrix} \begin{bmatrix} I & -A_{G:11}^{-1}A_{G:12} \\ 0 & I \end{bmatrix}$$

Since there is no overlap of the central element (no common interior DOF) of different macro superelements G , the exact elimination of interior unknowns in the global system can be done locally, i.e., for each macro superelement separately. For the transformation of the local matrices B_G associated with the reduced macro superelements, as depicted in Figure 5, we use a local harmonic interpolation of the remaining fine DOF subject to the compatibility constraint that the fine DOF of a given element are allowed to interpolate only from the coarse DOF of its attached elements. The corresponding faces are indicated by bold lines. Using Figure 5 for further explanation, this means

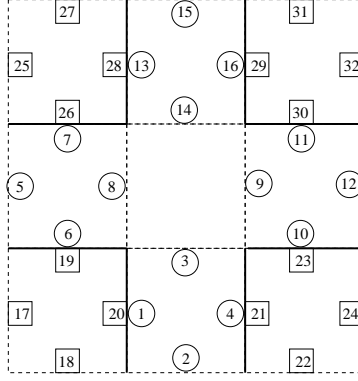


Figure 5: Degrees of freedom of reduced macro superelement

for instance that the DOF with local numbers 1, 2, 3, 4 are allowed to interpolate from the coarse DOF with numbers 17, 18, ..., 24 only. In order to construct a local harmonic interpolation, we assemble an auxiliary matrix C_G from those face matrices (corresponding to the bold lines) that originally produce the coupling of the remaining fine DOF (local numbers 1 to 16) with the coarse DOF (local numbers 17 to 32); Accordingly the matrix C_G is partitioned into 2×2 blocks of size 16×16 , i.e.,

$$C_G = \begin{bmatrix} C_{G:11} & C_{G:12} \\ C_{G:21} & C_{G:22} \end{bmatrix}.$$

A two-level splitting based on local energy minimization is then induced by the transformation matrix J_G^{EM} that is given as the product of two transformation steps, namely the static condensation

$$J_G^{\text{SC}} = \begin{bmatrix} I & P_G^{\text{SC}} & 0 \\ 0 & I & 0 \\ 0 & 0 & I \end{bmatrix} := \begin{bmatrix} I & -A_{G:11}^{-1} A_{G:12} & 0 \\ 0 & I & 0 \\ 0 & 0 & I \end{bmatrix}, \quad (10)$$

and the harmonic interpolation

$$J_G^{\text{HI}} = \begin{bmatrix} I & 0 & 0 \\ 0 & I & P_G^{\text{HI}} \\ 0 & 0 & I \end{bmatrix} := \begin{bmatrix} I & 0 & 0 \\ 0 & I & -C_{G:11}^{-1} C_{G:12} \\ 0 & 0 & I \end{bmatrix}, \quad (11)$$

that is,

$$J_G^{\text{EM}} = J_G^{\text{SC}} J_G^{\text{HI}} = \begin{bmatrix} I & -A_{G:11}^{-1} A_{G:12} & A_{G:11}^{-1} A_{G:12} C_{G:11}^{-1} C_{G:12} \\ 0 & I & -C_{G:11}^{-1} C_{G:12} \\ 0 & 0 & I \end{bmatrix}. \quad (12)$$

Note that the block $-A_{G:11}^{-1} A_{G:12}$ in the position (1,2) of (12) has no effect on the angle between the coarse and its complementary space. Hence, without loss of generality, we replace this block with the matrix of all zeros. Then, the final splitting based on local energy minimization is induced by a transformation of the form (9), where the local interpolation operator is given by

$$P_G = P_G^{\text{EM}} := \begin{bmatrix} P_G^{\text{SC}} P_G^{\text{HI}} \\ P_G^{\text{HI}} \end{bmatrix} := \begin{bmatrix} A_{G:11}^{-1} A_{G:12} C_{G:11}^{-1} C_{G:12} \\ -C_{G:11}^{-1} C_{G:12} \end{bmatrix}. \quad (13)$$

4.2 Two-level transformation with limiting interpolation weights

In practical computations the global two-level basis transformation that is induced by the local transformation (9) where P_G is given by (13) can easily be implemented. However, the matrix (13) certainly depends on the size of the stabilization parameter α in (4) and also on the (scalar) coefficient $a = a(T)$, which is assumed to be piecewise constant with (possible) jump discontinuities at the interior element interfaces on the finest mesh, here. Let us therefore consider a general macro super-element with piecewise constant coefficients a_1, a_2, \dots, a_9 , where $0 < a_i \leq 1$, see Figure 6. In

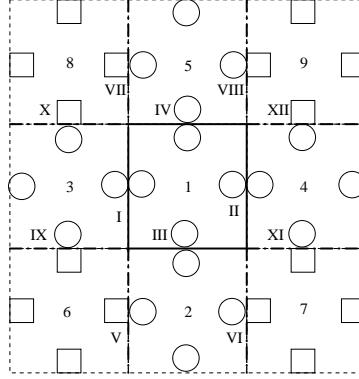


Figure 6: Local element and face numbering

the following we will define a parameter-free local two-level transformation for which it is possible to conduct a rigorous analysis that will be presented in Section 5. However, we want to stress that this is mainly for the purpose of gaining the theoretical insight.

Let us start our considerations with the building blocks of the interpolation matrix (13) which for the considered model problem are to be found

$$P_G^{\text{SC}} = P_G^{\text{SC}}(\alpha; a_1, a_2, \dots, a_9) := -A_{G:11}^{-1} A_{G:12} = P_{G,\infty}^{\text{SC}} + P_{G,\star}^{\text{SC}}(\alpha; a_1, a_2, \dots, a_9), \quad (14)$$

where

$$P_{G,\infty}^{\text{SC}} = \frac{1}{96} \begin{bmatrix} 7 & -1 & 3 & -5 & 1 & -1 & -1 & 81 & 9 & -1 & -1 & 1 & 7 & 3 & -1 & -5 \\ -1 & 1 & 81 & -1 & -1 & 7 & -5 & 3 & 3 & 7 & -5 & -1 & -1 & 9 & 1 & -1 \\ -1 & 1 & 9 & -1 & -1 & -5 & 7 & 3 & 3 & -5 & 7 & -1 & -1 & 81 & 1 & -1 \\ -5 & -1 & 3 & 7 & 1 & -1 & -1 & 9 & 81 & -1 & -1 & 1 & -5 & 3 & -1 & 7 \end{bmatrix}, \quad (15)$$

$$P_{G,\star}^{\text{SC}} = \frac{1}{96\alpha} \begin{bmatrix} 3a_2 & -a_2 & 60a_1 - 5a_2 & 3a_2 & -20a_3 & 60a_3 & 60a_3 & -4(24a_1 + 25a_3) \\ 60a_2 & -20a_2 & -4(24a_1 + 25a_2) & 60a_2 & -a_3 & 3a_3 & 3a_3 & 60a_1 - 5a_3 \\ 6a_2 & -2a_2 & -2(12a_1 + 5a_2) & 6a_2 & -a_3 & 3a_3 & 3a_3 & 60a_1 - 5a_3 \\ 3a_2 & -a_2 & 60a_1 - 5a_2 & 3a_2 & -2a_3 & 6a_3 & 6a_3 & -2(12a_1 + 5a_3) \\ -2(12a_1 + 5a_4) & 6a_4 & 6a_4 & -2a_4 & 3a_5 & 60a_1 - 5a_5 & -a_5 & 3a_5 \\ 60a_1 - 5a_4 & 3a_4 & 3a_4 & -a_4 & 6a_5 & -2(12a_1 + 5a_5) & -2a_5 & 6a_5 \\ 60a_1 - 5a_4 & 3a_4 & 3a_4 & -a_4 & 60a_5 & -4(24a_1 + 25a_5) & -20a_5 & 60a_5 \\ -4(24a_1 + 25a_4) & 60a_4 & 60a_4 & -20a_4 & 3a_5 & 60a_1 - 5a_5 & -a_5 & 3a_5 \end{bmatrix}, \quad (16)$$

and

$$P_G^{\text{HI}} = P_G^{\text{HI}}(\alpha; a_1, a_2, \dots, a_9) := -C_{G:11}^{-1} C_{G:12}. \quad (17)$$

First we note that the coefficients a_6 to a_9 do not appear in (16) at all. Moreover, and this is the important observation in the present context, we have

$$\lim_{\alpha \rightarrow \infty} P_G^{\text{SC}}(\alpha; a_1, a_2, \dots, a_9) = P_{G,\infty}^{\text{SC}} \quad (18)$$

showing that the interpolation matrix P_G^{SC} will be close to $P_{G,\infty}^{\text{SC}}$ for any (fixed) coefficient distribution if the stabilization parameter α is chosen large enough, i.e., the limit does not depend on any of the parameters a_i , $i = 1, \dots, 9$. Dealing with the matrix P_G^{HI} the expressions for the entries are more complicated as compared to P_G^{SC} , however, again the limit for $\alpha \rightarrow \infty$ is a constant matrix, i.e.,

$$\lim_{\alpha \rightarrow \infty} P_G^{\text{HI}}(\alpha; a_1, a_2, \dots, a_9) = P_{G,\infty}^{\text{HI}} \quad (19)$$

where

$$P_{G,\infty}^{\text{HI}} = \frac{1}{4} \begin{bmatrix} 0 & 0 & 0 & 4 & 0 & 0 & 0 & 0 & 0 & 0 & 0 & 0 & 0 & 0 & 0 \\ -1 & 2 & 0 & 1 & 1 & 2 & 0 & -1 & 0 & 0 & 0 & 0 & 0 & 0 & 0 \\ -1 & 0 & 2 & 1 & 1 & 0 & 2 & -1 & 0 & 0 & 0 & 0 & 0 & 0 & 0 \\ 0 & 0 & 0 & 0 & 4 & 0 & 0 & 0 & 0 & 0 & 0 & 0 & 0 & 0 & 0 \\ 2 & -1 & 1 & 0 & 0 & 0 & 0 & 0 & 2 & 1 & -1 & 0 & 0 & 0 & 0 \\ 0 & 0 & 4 & 0 & 0 & 0 & 0 & 0 & 0 & 0 & 0 & 0 & 0 & 0 & 0 \\ 0 & 0 & 0 & 0 & 0 & 0 & 0 & 0 & 0 & 4 & 0 & 0 & 0 & 0 & 0 \\ 0 & -1 & 1 & 2 & 0 & 0 & 0 & 0 & 0 & 1 & -1 & 2 & 0 & 0 & 0 \\ 0 & 0 & 0 & 0 & 2 & -1 & 1 & 0 & 0 & 0 & 0 & 2 & 1 & -1 & 0 \\ 0 & 0 & 0 & 0 & 0 & 0 & 4 & 0 & 0 & 0 & 0 & 0 & 0 & 0 & 0 \\ 0 & 0 & 0 & 0 & 0 & 0 & 0 & 0 & 0 & 0 & 0 & 0 & 4 & 0 & 0 \\ 0 & 0 & 0 & 0 & 0 & -1 & 1 & 2 & 0 & 0 & 0 & 0 & 0 & 1 & -1 & 2 \\ 0 & 0 & 0 & 0 & 0 & 0 & 0 & 0 & 0 & 0 & 0 & 4 & 0 & 0 & 0 & 0 \\ 0 & 0 & 0 & 0 & 0 & 0 & 0 & 0 & -1 & 2 & 0 & 1 & 1 & 2 & 0 & -1 \\ 0 & 0 & 0 & 0 & 0 & 0 & 0 & 0 & -1 & 0 & 2 & 1 & 1 & 0 & 2 & -1 \\ 0 & 0 & 0 & 0 & 0 & 0 & 0 & 0 & 0 & 0 & 0 & 4 & 0 & 0 & 0 & 0 \end{bmatrix}. \quad (20)$$

This allows us to define a two-level basis transformation of the form (9) via the local matrix

$$P_G = P_G^{\text{LW}} = P_{G,\infty}^{\text{EM}} := \begin{bmatrix} P_{G,\infty}^{\text{SC}} & P_{G,\infty}^{\text{HI}} \\ & P_{G,\infty}^{\text{HI}} \end{bmatrix} \quad (21)$$

where the building blocks $P_{G,\infty}^{\text{SC}}$ and $P_{G,\infty}^{\text{HI}}$ are given by (15) and (20), respectively. In particular, these interpolation matrices are parameter-free and the final two-level hierarchical basis representation of the global stiffness matrix (resulting from the related transformation) is based on *limiting interpolation weights*. Since the limit for $\alpha \rightarrow \infty$ exists for all of the involved (matrix-valued) functions we have the following lemma.

Lemma 4.1 *The limit for $\alpha \rightarrow \infty$ of the transformation based on local energy minimization (see (13)) is given by (9) where P_G is chosen according to (21), i.e.,*

$$\lim_{\alpha \rightarrow \infty} P_G^{\text{EM}}(\alpha; a_1, a_2, \dots, a_9) = P_G^{\text{LW}}. \quad (22)$$

The splitting obtained via the transformation (9) with specification (21) will be further studied in Section 5.

4.3 Multilevel generalized hierarchical basis

In the framework of hierarchical basis multilevel methods, in particular for algebraic multilevel iteration (AMLI) methods, a recursive (multilevel) extension of the considered two-level transformation is required. This is usually achieved by defining a two-level splitting – like the one considered in Section 4.1 – at each level, starting at level ℓ associated with the finest (original) finite element mesh, proceeding with level $\ell - 1$, and so forth, going down as far as level 1, the last but one coarse level. Then the multilevel basis transformation can be defined simply as the superposition of all two-level transformations, each of which is acting only on the remaining DOF.

In our case the global two-level transformation is always induced by a local transformation of the type (9). This means that the restriction of the global transformation $J^{(k)}$ at a given level k , $\ell \geq k > 0$, to the individual macro superelements G formed at this level is identical to the local transformation matrices J_G , which we collect in the set $\mathcal{J}^{(k)} := \{J_G : G \subset \mathcal{T}_k\}$ for the mesh partition \mathcal{T}_k . The construction of course goes the opposite direction, that is, the entries of the global matrix $J^{(k)}$ are determined by the set $\mathcal{J}^{(k)}$, i.e.,

$$J^{(k)}|_G := J_G \quad \forall G \subset \mathcal{T}_k.$$

Since this is not a standard assembling process we say that the local transformation, if known globally, induces the global transformation. Hence, only the nonzero pattern of J_G is predetermined and the entries of J_G , which in general change from one macro superelement to the next, have to be computed dynamically in this setting. In order to be able to compute the entries of an arbitrary element J_G of $\mathcal{J}^{(k)}$, the contributions associated with (interior) faces at level k have to be known globally. In practice, these individual face matrices at level k can be generated by computing local Schur complements from small-sized local matrices assembled from face matrices at level $k + 1$. For instance, assembling the two level- $(k + 1)$ face matrices that correspond to the overlap of two macro superelements that are attached to each other and eliminating in this assemblage the fine DOF results in a proper level- k face matrix. This process is illustrated by Figure 7 for a(n abstract) coarse face that is made up of two horizontal fine faces. If we denote by $A_{e_b}^{(k+1)}$ and by $A_{e_t}^{(k+1)}$ the level- $(k + 1)$ face matrices

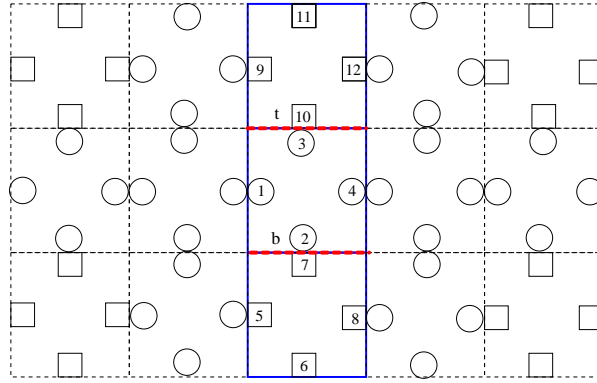


Figure 7: Generation of coarse face matrices

corresponding to a bottom face e_b and to a top face e_t such that they interconnect the two sets of DOF with local numbers $\{5, 6, 7, 8, 1, 2, 3, 4\}$ and $\{1, 2, 3, 4, 9, 10, 11, 12\}$, respectively, then their assemblage is $\tilde{A}_e^{(k+1)} := A_{e_b}^{(k+1)} + A_{e_t}^{(k+1)}$, and a level- k face matrix is obtained by elimination of the

fine DOF with local numbers $\{1, 2, 3, 4\}$ whose interconnection is represented by $\tilde{A}_{e:11}^{(k+1)}$ i.e.,

$$A_e^{(k)} := \tilde{A}_{e:22}^{(k+1)} - \tilde{A}_{e:21}^{(k+1)} (\tilde{A}_{e:11}^{(k+1)})^{-1} \tilde{A}_{e:12}^{(k+1)},$$

see Figure 7.

Thus the general procedure is as follows: First compute the face matrices and determine the global two-level transformation $J^{(\ell)}$ at level ℓ from the local transformation matrices $J_G \in \mathcal{J}^{(\ell)}$ (which do not need to be stored) by looping over all macro superelements $G \subset \mathcal{T}_\ell$. Next compute all face matrices at level $(\ell - 1)$ (from the face matrices at level ℓ); Then loop over the macro superelements at level $(\ell - 1)$ thereby computing one by one the local transformation matrices $J_G \in \mathcal{J}^{(\ell-1)}$ and assign their entries to the correct positions of $J^{(\ell-1)}$. Continue in this way for one level after the other, ending with the computation of $J^{(1)}$ at the second coarsest level with index 1.¹

5 Analysis of the two-level splitting

The construction of optimal preconditioners in the framework of multilevel block factorization is based upon a theory in which the constant γ in the so-called strengthened Cauchy-Bunyakowski-Schwarz (CBS) inequality plays a key role. The CBS constant measures the cosine of the abstract angle between the coarse space and its complementary space. The general idea is to construct a proper splitting by means of a (generalized) hierarchical basis transformation. The question whether the splitting introduced in the previous section is robust with respect to high coefficient variation will be answered after a short general introduction on local estimation of γ .

5.1 Local estimates for the CBS constant

In the hierarchical bases context we denote by \mathcal{V}_1 and \mathcal{V}_2 subspaces of the finite element space \mathcal{V}_h . The space \mathcal{V}_2 is spanned by the coarse-space basis functions and \mathcal{V}_1 is the complement of \mathcal{V}_2 in \mathcal{V}_h , i.e., \mathcal{V}_h is a direct sum of \mathcal{V}_1 and \mathcal{V}_2 :

$$\mathcal{V}_h = \mathcal{V}_1 \oplus \mathcal{V}_2$$

We want to emphasize that instead of computing the coarse-space basis explicitly, a (generalized) hierarchical basis can always be defined (implicitly) by specifying the related hierarchical basis transformation. The fact that we construct the global transformation based on the set of compatible local transformations ensures that the coarse-space basis functions have a local support; Even the sparsity pattern of the original stiffness matrix (with respect to the standard nodal basis) is reproduced by the resulting coarse-level matrix that typically serves as an approximation to the global Schur complement.

Let us consider our scalar second-order elliptic model problem. We first note that the following well-known definition of the strengthened CBS inequality constant

$$\gamma = \cos(\mathcal{V}_1, \mathcal{V}_2) = \sup_{u \in \mathcal{V}_1, v \in \mathcal{V}_2} \frac{A(u, v)}{\sqrt{A(u, u)A(v, v)}}$$

holds where $A(\cdot, \cdot)$ is the bilinear form that appears in the IP-DG finite element formulation (3). As it was shown in [2], the constant γ can be estimated locally, in our case over each macro superelement

¹For the coarsest level 0 we don't need a splitting into a(nother) coarse space and its complement.

G , which means that $\gamma = \max_G \gamma_G$, where

$$\gamma_G = \sup_{u \in \mathcal{V}_1(G), v \in \mathcal{V}_2(G)} \frac{\mathcal{A}_G(u, v)}{\sqrt{\mathcal{A}_G(u, u)\mathcal{A}_G(v, v)}}, \quad v \neq \text{const.}$$

The spaces $\mathcal{V}_k(G)$ above contain the functions from \mathcal{V}_k restricted to G and $\mathcal{A}_G(u, v)$ corresponds to $\mathcal{A}(u, v)$ restricted over the macro superelement G . We stress here, that the above technique has originally been developed for conforming finite elements; However, it can also be applied successfully to DG-nonconforming approximations, e.g., utilizing the construction of overlapping macro superelements, see Section 4. Moreover, the proposed approach is not limited to scalar problems.

The local analysis of the CBS constant is based on the following simple general rule to compute γ_G , see, e.g., [12, 20]:

$$\gamma_G^2 = 1 - \mu_1,$$

where μ_1 is the minimal eigenvalue of the generalized eigenproblem

$$S_G \mathbf{v}_{G:2} = \mu \hat{A}_{G:22} \mathbf{v}_{G:2}, \quad \mathbf{v}_{G:2} \notin \ker(\hat{A}_{G:22}). \quad (23)$$

Here $\hat{A}_{G:22}$ denotes the lower-right block of the hierarchical macro-superelement matrix (8) obtained via either of the local transformations J_G^{EM} or J_G^{LW} . In case of the scalar elliptic problem, $\hat{A}_{G:22}$ is of size 16×16 and its one-dimensional kernel is spanned by the constant vector, i.e.,

$$\ker(\hat{A}_{G:22}) = \text{span}\{(1, 1, \dots, 1)^t\}.$$

5.2 The case of highly varying coefficients

Let us come back to our model problem with highly varying coefficients. Our aim is to prove in this section for the two-level transformation with limiting interpolation weights, see Section 4.2, that the local CBS constant γ_G is uniformly bounded by some constant $c < 1$ for a general macro superelement matrix \hat{A}_G that stems from a problem with piecewise constant coefficient $a = a(T)$. Note that a on the discrete level without loss of generality can be represented by the coefficients a_1, a_2, \dots, a_9 , where $0 < a_i \leq 1$, cf. Figure 6.

If one tries to conduct the analysis according to the standard approach as outlined above, one runs into difficulties because the (symbolic) solution of the generalized eigenproblem (23) is extremely difficult due to the dependence of the matrices S_G and $\hat{A}_{G:22}$ of too many parameters. Already the computation of the parameter-dependent Schur complement S_G seems to be out of reach. That is why we use a different approach here.

Let us first recall the following important property of the (local) Schur complement S_G in (23), which is related to energy minimizing interpolation, that is, we have

$$\mathbf{v}_{G:2}^T S_G \mathbf{v}_{G:2} = \min_{\mathbf{v}_{G:1}} \begin{pmatrix} \mathbf{v}_{G:1} \\ \mathbf{v}_{G:2} \end{pmatrix}^T \begin{bmatrix} A_{G:11} & A_{G:12} \\ A_{G:21} & A_{G:22} \end{bmatrix} \begin{pmatrix} \mathbf{v}_{G:1} \\ \mathbf{v}_{G:2} \end{pmatrix} \quad \forall \mathbf{v}_{G:2} \quad (24)$$

where

$$A_G = \begin{bmatrix} A_{G:11} & A_{G:12} \\ A_{G:21} & A_{G:22} \end{bmatrix}$$

represents the fine-coarse partitioned macro superelement matrix A_G in the standard (nodal) basis. In the following we are concerned with proving a lower bound $\underline{\mu}$ for the minimal eigenvalue μ_1 of (23). We therefore rewrite

$$\mathbf{v}_{G:2}^T S_G \mathbf{v}_{G:2} \geq \underline{\mu} \mathbf{v}_{G:2}^T \hat{A}_{G:22} \mathbf{v}_{G:2} \quad \forall \mathbf{v}_{G:2}$$

in the form

$$\min_{\mathbf{v}_{G:1}} \begin{pmatrix} \mathbf{v}_{G:1} \\ \mathbf{v}_{G:2} \end{pmatrix}^T \begin{bmatrix} A_{G:11} & A_{G:12} \\ A_{G:21} & A_{G:22} - \underline{\mu} \hat{A}_{G:22} \end{bmatrix} \begin{pmatrix} \mathbf{v}_{G:1} \\ \mathbf{v}_{G:2} \end{pmatrix} \geq 0 \quad \forall \mathbf{v}_{G:2}. \quad (25)$$

So let us denote by B the matrix in (25), i.e.,

$$B := \begin{bmatrix} A_{G:11} & A_{G:12} \\ A_{G:21} & A_{G:22} - \underline{\mu} \hat{A}_{G:22} \end{bmatrix}. \quad (26)$$

If we are able to show that B is symmetric positive semidefinite (SPSD) for a given constant $\underline{\mu} > 0$ then $\underline{\mu}$ provides a lower bound for μ_1 .

We are ready to prove the main result of this section.

Theorem 5.1 Consider the general macro superelement matrix \hat{A}_G obtained via (8) where the two-level transformation J_G is based on interpolation with limiting weights, see (21), and the matrix A_G stems from local assembling of the face matrices (5) and (6) with piecewise constant coefficient $a(T)$ over the macro superelement, i.e., $a_i \in (0, 1]$, $1 \leq i \leq 9$. If $\alpha \geq \alpha_0 = 25$ then we have the bound

$$\gamma_G^2 \leq \frac{3}{4} \quad (27)$$

independent of the coefficient jumps that means for any choice of $a_i \in (0, 1]$.

Proof The particular construction of the interpolation (21) with constant interpolation weights implies that the matrix B defined in (26) takes the form

$$B = B(\alpha; \mu; a_1, \dots, a_9) = \alpha (B_0 + \mu C_0) + \sum_{i=1}^9 a_i (B_i + \mu C_i) \quad (28)$$

with constant matrices B_i and C_i for $i = 0, \dots, 9$. The matrices B_0 and C_0 are to be found SPSPD and indefinite, respectively. Moreover, a direct computation shows that $B_0 + \mu C_0$ is SPSPD for any $\mu \leq \mu_0 = (821 - \sqrt{27129})/1064 \approx 0.616815$. Hence $B_0 + \mu C_0$ is SPSPD for $\mu = 1/4$. If for a fixed $\mu \leq \mu_0$ and a fixed stabilization parameter $\alpha = \alpha_0$ there holds $B(\alpha_0; \mu; a_1, \dots, a_9) \geq 0$ then clearly $B(\alpha; \mu; a_1, \dots, a_9)$ is SPSPD for all $\alpha \geq \alpha_0$ for the same value of μ . Thence it suffices to prove that

$$B(\alpha_0; \underline{\mu}; a_1, \dots, a_9) \geq 0 \quad (29)$$

for a given pair $(\alpha_0, \underline{\mu})$ in order to conclude that the inequality (25) holds for any $\alpha \geq \alpha_0$. Now, assuming that $\alpha = \alpha_0$ and $\mu = \underline{\mu}$ are fixed, the matrix B according to (28) depends linearly on the parameters $a_i \in (0, 1]$. Thus we have

$$\begin{aligned} \min_{\mathbf{v}_G \neq \mathbf{0}} \left(\min_{a_i \in (0,1]} \frac{\mathbf{v}_G^t B(\alpha_0; \underline{\mu}; a_1, \dots, a_9) \mathbf{v}_G}{\mathbf{v}_G^t \mathbf{v}_G} \right) &\geq \min_{\mathbf{v}_G \neq \mathbf{0}} \left(\min_{a_i \in \{0,1\}} \frac{\mathbf{v}_G^t B(\alpha_0; \underline{\mu}; a_1, \dots, a_9) \mathbf{v}_G}{\mathbf{v}_G^t \mathbf{v}_G} \right) \\ &= \min_{a_i \in \{0,1\}} \left(\min_{\mathbf{v}_G \neq \mathbf{0}} \frac{\mathbf{v}_G^t B(\alpha_0; \underline{\mu}; a_1, \dots, a_9) \mathbf{v}_G}{\mathbf{v}_G^t \mathbf{v}_G} \right) \\ &= \min_{a_i \in \{0,1\}} \lambda_{\min}(B(\alpha_0; \underline{\mu}; a_1, \dots, a_9)). \end{aligned} \quad (30)$$

Finally, since for $\alpha_0 = 25$ and $\underline{\mu} = 1/4$ the minimal eigenvalue of $B(\alpha_0; \underline{\mu}; a_1, \dots, a_9)$ equals 0 for any choice of $a_i \in \{0, 1\} \forall i = 1, \dots, 9$ the bound (27) holds. \blacksquare

Remark 5.1 The bound (27) holds with strict inequality, too, because the pair $(\alpha_0, \underline{\mu}) = (25, 0.251)$ can also be used in the above line of argument. In fact, even smaller upper bounds are obtained for γ_G when using larger values of α_0 .

Remark 5.2 The condition to be met for optimal order multilevel methods, which are based on the multiplicative two-level preconditioner, is

$$\frac{1}{\sqrt{1 - \gamma^2}} < \beta < \varrho.$$

Since the reduction factor of the number of DOF in our case is $\varrho \approx 4$, we conclude that we can afford up to third degree polynomial stabilization in this setting. For second degree polynomials, or, alternatively, for two inner iterations at every (intermediate) level, the method will be of optimal order if $\gamma^2 < 3/4$.

6 Numerical study of the CBS constant

The background of this work are multilevel methods that are based on a recursive application of certain two-level methods. Here we investigate robustness issues for particular splittings of certain DG-nonconforming approximations. As the classical theory predicts, efficient two- and multilevel preconditioners can be constructed based on such splittings if the CBS-constant γ is strictly less than 1. Considering the particular splittings that have been presented in Section 4 the numerical experiments described in the rest of this section are devoted to the verification of this important property.

6.1 Constant coefficients

In the first experiment we compute recursively the squared local CBS constant γ_G^2 for the scalar elliptic problem with constant coefficients. Each time the lower-right 16×16 block of the matrix \hat{A}_G in (8) is used to assemble a new macro superelement matrix A_G that can be associated with the next coarser level then. Figure 8 depicts the multilevel behavior, i.e., the value of γ_G^2 on the first 15 levels, for the transformation based on local energy minimizing interpolation (12) and different values of the stabilization parameter α .

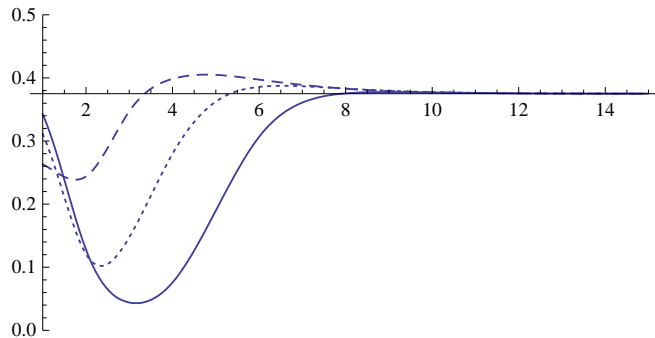


Figure 8: Multilevel behavior of γ_G^2 for constant coefficients: $\alpha = 10$ (dashed); $\alpha = 100$ (dotted); $\alpha = 1000$ (solid)

It is evident that the angle between the two subspaces is uniformly bounded from below in the multilevel setting. Of course, the sequence of recursively computed local γ -values in general depends on the choice of α . The results plotted in Figure 8 are for $\alpha \in \{10, 100, 1000\}$. Moreover, it is interesting to note that the CBS constant converges to $\sqrt{3/8}$ for any reasonable choice of α , e.g., for $\alpha > (\sqrt{23329} - 127)/8$, cf. Remark 3.1.

6.2 Random coefficients

In the following experiment we compute the value of the squared local CBS constant γ_G^2 for the case of random jumps in the coefficients on the macro superelement for different choices of the stabilization parameter α , i.e., $\alpha \in \{10, 100, 1000\}$. Again, the computations are carried out for the splitting based on local energy minimizing interpolation, cf. (12), and this time also for the transformation based on limiting interpolation weights J_G^{LW} , cf. (9) and (21).

The configuration is a stochastically independent (uniformly distributed) random value of the diffusion coefficient in the interval $(0, 1)$ for each element, i.e., a set of nine random numbers in $(0, 1)$ for the (reference) super macroelement. Then 100 randomly generated sets of random coefficients are considered and γ_G^2 is evaluated twice for each such set and each choice of the parameter α . The first value—illustrated by the dashed lines in Figures 9–11—corresponds to the limiting transformation J_G^{LW} , the second—illustrated by solid lines—corresponds to (12).

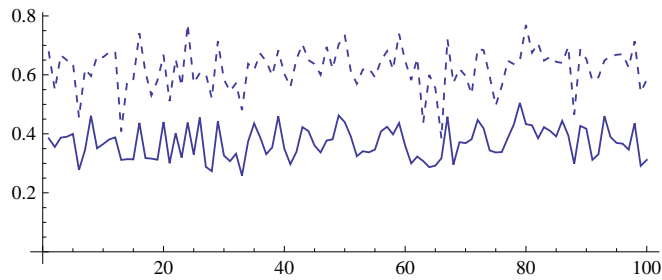


Figure 9: Two-level behavior of γ_G^2 for random coefficients; $\alpha = 10$: J_G^{LW} (dashed); J_G^{EM} (solid)

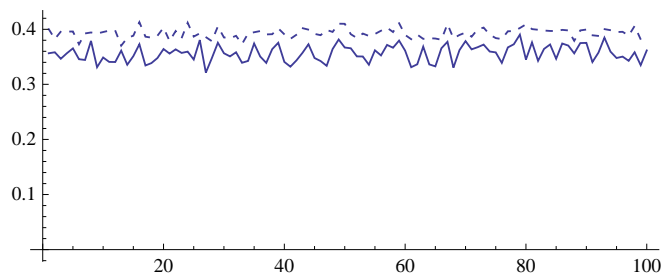


Figure 10: Two-level behavior of γ_G^2 for random coefficients; $\alpha = 100$: J_G^{LW} (dashed); J_G^{EM} (solid)

The results plotted in Figures 9–11 show that the local CBS constant is always nicely bounded away from 1 for both transformation variants. However, the *true* local energy minimization provides

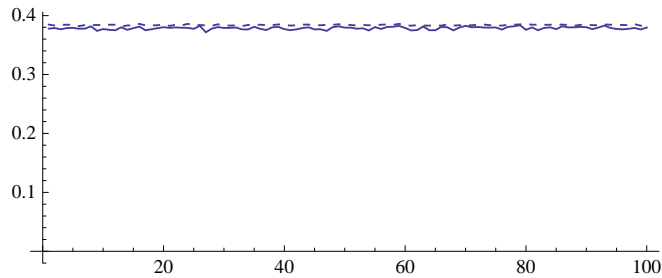


Figure 11: Two-level behavior of γ_G^2 for random coefficients; $\alpha = 1000$: J_G^{LW} (dashed); J_G^{EM} (solid)

the better splitting (the smaller CBS constant) in all our test cases. Whereas the observed values for γ_G^2 are much larger for the transformation based on limiting interpolation weights (dashed lines) when α is small, see Figure 9, the results significantly improve when increasing the stabilization parameter; As expected, for $\alpha = 1000$ there is almost no difference between both two-level splittings, see Figure 11. We further observe that the variation of γ_G^2 depends on α . It is smaller for larger α in general.

7 Concluding remarks

In this paper we presented a new construction of robust hierarchical splittings (two-level transformations) in the framework of generalized hierarchical bases for discontinuous Galerkin finite element discretizations of elliptic problems. The starting point was a particular splitting of the (local) bilinear form into contributions associated with element (inter)faces. This allowed us to set up for every level of mesh refinement an overlapping partition into superelements and macro superelements and to compute also the corresponding local stiffness matrices. A local transformation was then defined based on energy minimizing interpolation on macro superelement level, which induces the global two-level transformation. The consideration of limiting interpolation weights gave some first theoretical insight, i.e., it allowed us to derive a theoretical bound on the CBS constant, which is an important measure for the quality of the two-level splitting into a coarse space and its complement. To our knowledge this is the first result that extends the well-established theory of hierarchical basis multilevel methods to the case of elliptic problems with highly varying coefficients (arbitrary coefficient jumps on the fine mesh). The proposed approach is certainly neither limited to the particular family of Rannacher-Turek type elements nor to scalar elliptic problems nor to interior penalty DG formulations, as they have been considered in this paper.

8 Acknowledgments.

The authors gratefully acknowledge the support by the Austrian Academy of Sciences, the Bulgarian Academy of Sciences, and the Austrian Science Foundation, FWF Project P19170-N18.

References

- [1] D.N. Arnold and F. Brezzi, Mixed and non-conforming finite element methods: implementation, postprocessing and error estimates, *RAIRO, Model. Math. Anal. Numer.*, **19** (1985), 7-32.
- [2] O. Axelsson and I. Gustafsson, Preconditioning and two-level multigrid methods of arbitrary degree of approximations, *Math. Comp.*, **40** (1983), 219-242.
- [3] D. Arnold, F. Brezzi, B. Cockburn and L.D. Marini, Unified analysis of discontinuous Galerkin methods for elliptic problems, *SIAM J. Numer. Anal.*, **39** (2002), 1749–1779.
- [4] O. Axelsson and P.S. Vassilevski, Algebraic Multilevel Preconditioning Methods I, *Numer. Math.*, **56** (1989), 157-177.
- [5] O. Axelsson and P.S. Vassilevski, Algebraic Multilevel Preconditioning Methods II, *SIAM J. Numer. Anal.*, **27** (1990), 1569-1590.
- [6] R. Blaheta, S. Margenov and M. Neytcheva, Uniform estimate of the constant in the strengthened CBS inequality for anisotropic non-conforming FEM systems, *Numer. Lin. Alg. Appl.*, **11(4)** (2004), 309-326.
- [7] R. Blaheta, S. Margenov and M. Neytcheva, Robust optimal multilevel preconditioners for non-conforming finite element systems, *Numer. Lin. Alg. Appl.*, **12(5-6)** (2005), 495-514.
- [8] S. Brenner and J. Zhao, Convergence of multigrid algorithms for interior penalty methods, *Appl. Numer. Anal. Comput. Math.*, **2(1)** (2005), 3-18.
- [9] B. Cockburn, Discontinuous Galerkin methods, *Z. Angew. Math. Mech.*, **83(11)** (2003), 731-754.
- [10] V.A. Dobrev, R.D. Lazarov, P.S. Vassilevski and L.T. Zikatanov, Two-level preconditioning of discontinuous Galerkin approximations of second order elliptic equations, *Numer. Lin. Alg. Appl.*, **13(6)** (2006), 753-770.
- [11] V.A. Dobrev, R.D. Lazarov and L.T. Zikatanov, Preconditioning of symmetric interior penalty discontinuous Galerkin FEM for elliptic problems, *Domain Decomposition Methods in Science and Engineering XVII, Springer LNCSE*, **60** (2008), 33-44.
- [12] V. Eijkhout and P.S. Vassilevski, The Role of the Strengthened Cauchy-Bunyakowski-Schwarz Inequality in Multilevel Methods, *SIAM Review*, **33** (1991), 405-419.
- [13] R.E. Ewing, J. Wang, and Y. Yang, A stabilized discontinuous finite element method for elliptic problems, *Numer. Lin. Alg. Appl.*, **10(1-2)** (2003), 83-104.
- [14] R. Falgout, P.S. Vassilevski and L.T. Zikatanov, On two-grid convergence estimates, *Numer. Lin. Alg. Appl.*, **12** (2005), 471-494.
- [15] I. Georgiev, J. Kraus and S. Margenov, Multilevel preconditioning of 2D Rannacher-Turek FE problems; Additive and multiplicative methods, *Large-Scale Scientific Computing, Springer LNCS*, **4310** (2007), 56-64.

- [16] I. Georgiev, J. Kraus and S. Margenov, Multilevel preconditioning of rotated bilinear non-conforming FEM problems, *Computers & Mathematics with Applications*, **55** (2008), 2280-2294.
- [17] J. Gopalakrishnan and G. Kanschat, A multilevel discontinuous Galerkin method, *Numerische Mathematik*, **95(3)** (2003), 527-550.
- [18] P. Hansbo and M. Larson, A simple nonconforming bilinear element for the elasticity problem, *Trends in Computational Structural Mechanics, CIMNE*, (2001), 317-327.
- [19] T.J.R. Hughes, *The Finite Element Method: Linear Static and Dynamic Finite Element Analysis*, Prentice-Hall, New Jersey, 1987.
- [20] J. Kraus, S. Margenov, Multilevel methods for anisotropic elliptic problems, *Lectures on Advanced Computational Methods in Mechanics, Radon Series Comp. Appl. Math.*, **1** (2007), 47-87.
- [21] J. Kraus, S. Margenov, J. Synka, On the multilevel preconditioning of Crouzeix-Raviart elliptic problems, *Numer. Lin. Alg. Appl.*, **15** (2008), 395-416.
- [22] J. Kraus and S. Tomar, Multilevel preconditioning of two-dimensional elliptic problems discretized by a class of discontinuous Galerkin methods, *SIAM J. Sci. Comput.*, **30** (2008), 684-706.
- [23] J. Kraus and S. Tomar, A multilevel method for discontinuous Galerkin approximation of three-dimensional anisotropic elliptic problems, *Numer. Lin. Alg. Appl.*, **15** (2008), 417-438.
- [24] R.D. Lazarov and S.D. Margenov, CBS constants for multilevel splitting of graph-Laplacian and application to preconditioning of discontinuous Galerkin systems, *Journal of Complexity*, **23** (2007), 498-515.
- [25] R. Rannacher and S. Turek, Simple non-conforming quadrilateral Stokes Element, *Numerical Methods for Partial Differential Equations*, **8(2)** (1992), 97-112.